Hertz Elastic Contact in Spherical Nanoindentation Considering Infinitesimal Deformation of Indenter

Seung-Kyun Kang[*], Young-Cheon Kim[*], Yun-Hee Lee[**], Ju-Young Kim[***], Dongil Kwon[*]

[*]Department of Materials Science and Engineering, Seoul National University, Seoul 151-744, Korea, kskg7227@snu.ac.kr

[**]Division of Industrial Metrology, Korea Research Institute of Standards and Science, Daejeon 305-340, Korea, uni44@kriss.re.kr

[***]School of Mechanical & Advanced Materials Engineering, UNIST, Ulsan 689-798, Korea, juyoung@unist.ac.kr

ABSTRACT

The nanoindentation technique has made it possible to measure deformations at extremely low forces and displacements. Many studies have been performed to identify and analyze unusual nano-scale phenomena. The violation of Hertz elastic contact between a spherical nanoindenter and metallic materials has been discussed in previous studies. When a sharp indenter is used and elasto-plastic contact occurs, the elastic modulus is well predicted by elastic contact theory. However, since nanoindentation is widely used to measure elastic moduli of nano-size samples, unexpected results using a spherical indenter have raised doubt about elastic contact in nanoindentation. We performed fully elastic loading and unloading nanoindentation on fused silica. To characterize the actual geometry of the spherical indenter we measured it directly using an atomic-force microscope. We then confirmed the actual indenter radius in experiments by comparison to indenter radius measured from residual impression size above 200 nm indentation depth. The Hertz equation was found to underestimate the indentation depth. To understand this phenomenon, we reconsidered the frame compliance, which in general nannoindentation testing is taken as constant. The infinitesimal deformation of the spherical indenter was calculated by summing the partial compliances of the infinite cylinder of the indenter. We found that indenter compliance depends on indentation depth on a logarithmic scale. We adopted an indentation-depth-dependent frame compliance to evaluate accurate force and depth data for indentation depths less than 100 nm. The recalibrated curve is found to be identical to the Hertz equation.

Keywords: nanoindentation, Hertz contact, elastic contact, frame compliance

1 INTRODUCTION

Nanoindentation is widely used to characterize nano-scale materials such as thin films, coating layers, and metallic microstructures [1-6]. Compared to conventional macro indentation, nanoindentation has the advantage of measuring elastic response by monitoring the unloading response versus force and depth. Many studies [1-9] have shown the power of nanoindentation in measuring elastic modulus from the unloading curve, as well summarized by the Oliver-Pharr method [1].

On the other hand, hardness at the nano scale shows an unexpected deviation, the so-called indentation size effect (ISE). Hardness is considered a invarient value, but at nano scales it appears to increase as indentation depth decreases. This response has attracted interest and many studies have been performed to analyze the ISE by considering geometrically necessary dislocations [4-6]. In spite of this variation in hardness, it is generally accepted that the elastic modulus is derived from atomic bonding forces and is thus a constant.

The Oliver-Pharr method for evaluating elastic modulus is well verified for the Berkovich indenter, the indenter generally used in nanoindentation [1-6]. Recently, however, a deviation of elastic modulus from the Oliver-Pharr method, has been reported for spherical indentation [7,8,10]. The violation has also been reported in perfect elastic contact in spherical indentation, which does not use the Oliver-Pharr method [8]. This result is interesting because elastic contact theory was fundamentally derived from the contact of spherical bodies and results for a Berkovich indenter are estimated by deviation from a spherical indenter.

The apparent variation in elastic modulus for a spherical indenter could arise for two general reasons. One is the indenter shape problem. Even with improvements in the focused ion beam indenter manufacture, imperfections in the spherical shape are inevitable, and in addition the actual indenter raidus could differ from the manufacturer's nominal value. The second possibility is calibration of frame compliance. Nanoindentation techniques generally do not consider indenter compliance separately from total frame compliance. In this paper, we verify Hertz contact theory in perfect elastic contact conditions by calibrating actual indenter shape and frame compliance.

2 EXPERIMENTS

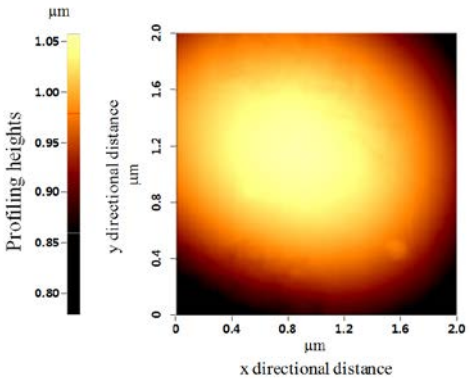

Figure 1: 3D profile of spherical indenter (top view) [8].

A diamond spherical indenter (Micro Star Technologies Inc., TX, USA) made by fabricating a conical indenter was prepared. The side-view TEM image of the indenter was used to estimate nominal indenter radius, 5 μm. A series of nanoindentations with spherical indenter was performed using the Nanoindenter XP (Agilent, USA). The elastic modulus and Poisson's ratio of fused silica were 72 GPa and 0.17, respectively. At 90 nm indentation depth, the loading and unloading curves are identical, so that the curves are reversible with perfect elastic contact. We used two methods to confirm the indenter shape. Atomic force microscopy (AFM, SIS NanostationII) was used for direct measurement of the indenter up to 80 nm indentation depth. The residual surface impression was measured by AFM over the 200 nm indentation depth, where plastic deformation occured. We prepared four metal samples, Al, Cu, Ni, and SCM4, of elastic moduli 70, 125, 200 and 210 GPa respectively, as measured by an ultrasonic pulse-echo technique for verification of frame compliance. Nanoindentation specimens were electroplished after mechanical polishing with 0.05 μm diamond powder to control the surface roughness.

3 INDENTER GEOMETRY

Figure 1 shows the 3D profile of the spherical indenter at indentation depths less than 90 nm. As the contour line is circular, we can say that the indenter has maintained its spherical shape. From the cross-sectional area (A) and indentation depth (h), the effective indenter radius (R) was calculated from:

$$R = \frac{(A/\pi) + h^2}{2h}. \qquad (1)$$

The effective radii derived by the two different methods are compared in Figure 2. The effective radius under 90 nm indentation was 4.40 ± 0.11 μm; that for depths over 200 nm was 4.84 ± 0.20 μm. the two do not match perfectly, but they show a regular increase within 10% deviation. Previous research [7] has shown that reliable elastic moduli

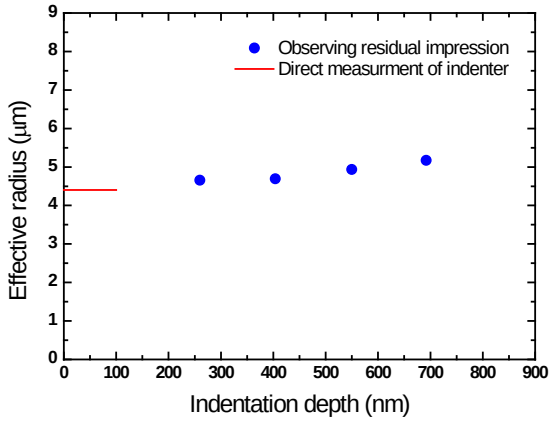

Figure 2: Effective radii derived by two different methods [8].

can be achieved by replacing the indenter radius by an effective radius.

4 FRAME COMPLIANCE

4.1 Perfect elastic contact

After adopting the effecitve radius we can derive a perfect elastic loading curve using the equation

$$P = \frac{4}{3} E_r \sqrt{R} h^{3/2}, \qquad (2)$$

where P is indentation load and E_r is reduced modulus [8,11]. This equation, known as the Hertz equation, is the solution for the contact of of perfect elastic bodies. As the nanoindentation test on fused silica was perfect elastic contact up to 90 nm, the indentation force and depth curve is expected to be identical to Hertz's solution. Figure 3 shows the indentation force and depth curve for fused silica. The loading and unloading curves are identical and can be considered perfect elastic contact. The straight line shows the Hertz equation using an effective radius and the elastic

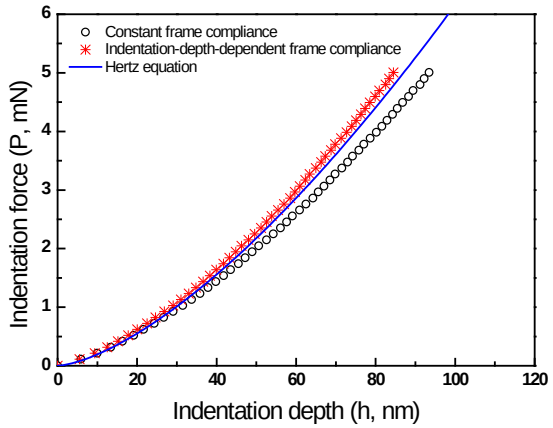

Figure 3: Hertz equation andndentation force-depth curve after calibrating frame compliances [8].

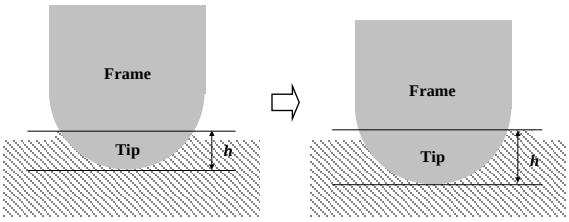

Figure 4: Change of contact and frame boundary (schematic) [7].

modulus measured from ultrasonic pulse-echo method. The Hertz equation significently overestimated the force found in the nanoindentation test. To resolve this mismatch we consider the infinitesimal deformation of indenter in the following section.

4.2 Indentation-depth-dependent compliance

During nanoindentation testing, the frame body, which transfers force from the actuating source to the sample, is also compressed. Unfortunately, displacement sensing based on the reference and difference method includes not only indentation depth but also the deformation of the frame body. For this reason following equations are used to predetermine and calibrate frame compliance:

$$\frac{1}{S_{total}} = C_{frame} + \frac{1}{S_{sample}}, \tag{3}$$

$$C_{frame} = \frac{1}{S_{total}} - \frac{\sqrt{\pi}}{2E_r\sqrt{A}}, \tag{4}$$

where S_{total} is the initial unloading stiffness from the indentation force-depth curve, C_{frame} is frame compliance and S_{sample} is sample stiffness [1,2,7,8]. By measuring cross-sectional area and elastic modulus of the sample and tip, we can derive frame compliance using Equation (4). In general, frame compliance is regarded as a system property of indentation equipment and is believed to be constant for a given setup.

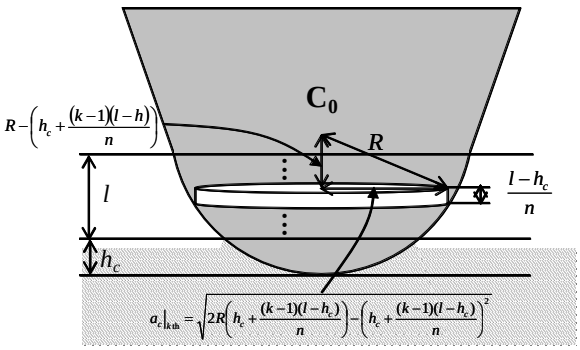

Figure 5: Calculation of frame compliance for unit frame [8].

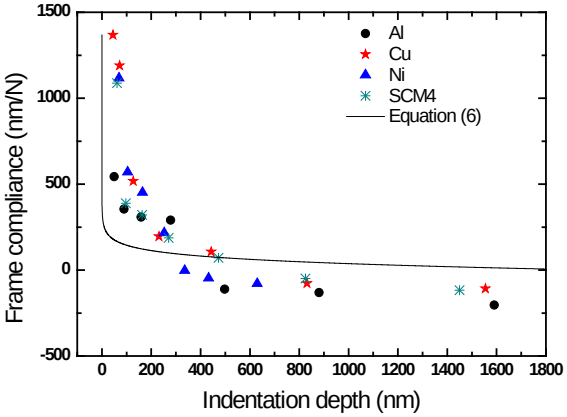

Figure 6: Variation in frame compliance as a function of indentation depth [8].

We have reviewed the concept of frame compliance focusing on the deformation of indenter. Figure 4 is a simple sketch of changes in the frame boundary with increasing indentation depth. We can say that only the indenter below the contact boundary is effective indenter and the other part does not affect to frame compliance. As indentation depth increases, the frame boundary moves toward the frame body and frame compliance decreases. To quantify the model we use the following definition of compliance (C) at the simple compression state:

$$C = \frac{1}{E}\cdot\frac{h^*}{A}, \tag{5}$$

where E is elastic modulus and h^* is the height of unit system [7,8]. The schematic diagram in Figure 5 represents the spherical indenter as a summation of infinite cylindrical units. By summing the infinite compliance of spherical indenter, the total frame compliance of indenter part ($C_{indenter}$) is expressed as

$$C_{indenter} = \frac{1}{E_t}\frac{1}{\pi}\frac{1}{2R}\ln\frac{l}{(2R-l)}\left(\frac{2R}{h}-1\right), \tag{6}$$

where E_t is the tip elastic modulus and l is the length of indenter [7,8].

To verify Equation (6) we directly calculate the frame compliance from Equation (4) for four metals: Al, Cu, Ni, and SCM4. Figure 6 shows the indentation-depth-dependent frame compliance derived from Equations (4) and (6). The frame compliance expressed by our model well predicts the decrease in hardness with increasing indentation depth.

4.3 Calibration of force-depth curve

As frame compliance is not a constant but a function of indentation depth, the following iteration is required to obtain actual indentation depth:

$$h^n = h^0 - f(h^{n-1})P, \quad (7)$$

where h^0 and P are the initial measured indentation depth and force, h^n is the nth calibrated indentation depth, and h^{n-1} is the indentation depth calculated from the (n-1)th calibration with Equation (6) [7,8]. We now use Equation (7) to reevaluate the actual indentation force and depth curve in Figure 3. As increasing of initial frame compliance, the indentation depth decreases after calibrating indentation-depth-dependent frame compliance. We also see that the newly derived curve is almost identical to the Hertz equation.

5 CONCLUSION

We have investigated the deviation from Hertz contact equation in nanoindentation with spherical indenter. Indenter shape was checked by direct measurement and AFM profiling of the residual impression. The force-depth curves are not identical to Hertz equation in spite of the indenter shape calibration. Frame compliance was then reviewed, focusing on the change of boundary between frame and sample, and the actual frame compliance was calculated by summating compliances of infinitesimal units. The reevaluated indentation force-depth curve was found to be identical to the Hertz equation.

REFERENCES

[1] W.C. Oliver and G.M. Pharr, J. Mater. Res. 7, 564, 1992.

[2] C. Ullner, E. Reimann, H. Kohlhoff and A. Subaric-Leitis, Measurement 43, 216, 2010..

[3] E.G. Herbert, G.M. Pharr, W.C. Oliver, B.N. Lucas and J.L. Hay, Thin Solid Films 398-399, 331, 2001.

[4] W.D. Nix and H. Gao, J. Mech. Phys. Sol. 46, 411, 1998.

[5] K.W. McElhaney, J.J. Vlassak, and W.D. Nix, J. Mater. Res. 13, 1300, 1998.

[6] H. Gao, Y. Huang, W.D. Nix, and J.W. Hutchinson, J. Mech. Phys. Sol. 47, 1239, 1999.

[7] S.K. Kang, J.Y. Kim, I. Kang, and D. Kwon, J. Mater. Res. 24, 2965, 2009.

[8] S.K. Kang, Y.C. Kim, Y.H. Lee, J.Y. Kim, and D. Kwon, Mater. Sci. Eng. A 538, 58, 2012.

[9] J.H. Ahn and D. Kwon, J. Mater. Res. 16, 3170, 2001.

[10] J. Rodríguez and M.A.G. Maneiro, Mech. Mater. 39, 987, 2007.

[11] H. Bei, E.P. George, J.L. Hay and G.M. Pharr, Phys. Rev. Lett. 95, 045501, 2005.